

Effect of mtDNA depletion from C6 glioma cells and characteristics of the generated C6p0 cells

YOUCAI JIN^{1,3}, GUANGXIANG LUAN^{1,3,4}, JI LI⁵, HONGLUN WANG^{1,4,5}, ZHENHUA WANG⁵ and BO BAI¹

¹Key Laboratory of Tibetan Medicine Research, Northwest Institute of Plateau Biology, Chinese Academy of Sciences;

²College of Chemistry and Chemical Engineering, Qinghai Normal University, Xining, Qinghai 810008;

³University of Chinese Academy of Sciences, Beijing 100049; ⁴Key Laboratory of Tibetan Medicine Research of Qinghai Province, Northwest Institute of Plateau Biology, Chinese Academy of Sciences, Xining, Qinghai 810008;

⁵Center for Mitochondria and Healthy Aging, College of Life Sciences, Yantai University, Yantai, Shandong 264005, P.R. China

Received April 25, 2020; Accepted December 8, 2020

DOI: 10.3892/mmr.2021.11904

Abstract. Malignant tumors of the central nervous system (CNS) are among the types of cancer with the poorest prognosis and glioma is the commonest primary CNS tumor. A mitochondrial DNA (mtDNA)-depleted cell line C6p0 was generated from C6 glioma cells after long-term exposure to ethidium bromide and 2',3'-dideoxycytidine in order to determine the effect of mtDNA damage on cell proliferation and pathological changes in glioma cells. Single cell clones were isolated and identified after 42 days of incubation. Repopulated cybrids were formed when the clonal C6p0 cells were fused with rat platelets and no difference was observed in their growth in a selective medium without uridine and pyruvate compared with the growth of the parent C6 cells. Disruption of mtDNA resulted in changes in mitochondrial morphology, decreased cell proliferation, reduced intracellular reactive oxygen species and intracellular ATP, along with decreased mtDNA and mitochondrial membrane potential in C6p0 cells compared with the C6 cells. Taken together, C6p0 cells without mtDNA were established for the first time and their characteristics were compared with parent cells. This C6p0 cell line could be used to explore the contribution of mitochondrial dysfunction and mtDNA mutations in the pathogenesis of glioma.

Introduction

Malignant tumors of the central nervous system (CNS) are among the types of cancer with the poorest prognosis, with high levels of morbidity and mortality (1). Glioma is the most common primary CNS tumor deriving from neuroglial stem or progenitor cells (2). Mitochondrial DNA (mtDNA) mutations have been found to be closely associated with various types of cancer, neurodegenerative disorders, attention-deficit hyperactivity disorder, headache, diabetes and aging (3-8). Therefore, a study on the effect of mtDNA heterogeneity on glioma growth, differentiation and death is required. Mitochondria serve a crucial and integral role in maintaining cell homeostasis, including energy synthesis, redox regulation, cell messaging and hematopoiesis (9,10) and they provide ~80-90% of the energy to the cell through the respiratory chain and this percentage reaches 95% in the heart (11,12). Furthermore, mitochondria regulate apoptosis and cell cycle through their role in several processes including calcium signaling, reactive oxygen species (ROS) homeostasis, biosynthesis of heme, biosynthesis of iron-sulfur clusters and tumorigenesis (13).

Since mtDNA mutations can compromise the mitochondrial function and lead to human pathologies, there is a strong and continuing interest in their role in human health and disease. Unfortunately, the study of mtDNA mutations is not easy due to the nuclear background diversity and the role it serves in the modulation of mitochondrial defects (14). Fortunately, hybrid technology provides a new strategy to study diseases associated with mitochondrial dysfunctions. The technique is based on the use of a cell line in which the mtDNA is depleted (p0 cells) and can be used as a mitochondrial receptor when fused with platelets (15,16). Since cytoplasmic hybrids (cybrids) have the same genetic background, biochemical analysis is made possible. Previous studies have demonstrated that ethidium bromide (EB), 2',3'-dideoxycytidine (ddC), rhodamine-6g, 1-methyl-4-phenylpyridinium, zidovudine and stavudine, together with NT2 human teratocarcinoma, T47d human breast cancer cells, 143B human bone osteosarcoma thymidine kinase negative (TK-) and human mesenchymal stem cell (3a6 and KP) are commonly used to produce p0 cells (13,17-19).

Correspondence to: Dr Bo Bai, Key Laboratory of Tibetan Medicine Research, Northwest Institute of Plateau Biology, Chinese Academy of Sciences, 23 Xinning Road, Xining, Qinghai 810008, P.R. China
E-mail: baibochina@163.com

Professor Zhenhua Wang, Center for Mitochondria and Healthy Aging, College of Life Sciences, Yantai University, 30 Qingquan Road, Yantai, Shandong 264005, P.R. China
E-mail: zhenhuawang@tom.com

Key words: C6 glioma, p0, mitochondrial DNA, cytoplasmic hybrids, mitochondrial

Therefore, in the present study, the mtDNA-depleted cell line C6 ρ 0 was generated from C6 glioma cells and the mtDNA-related deficits were determined. The results demonstrated that C6 ρ 0 cells could be a useful tool in the investigation of mitochondrial dysfunction and mtDNA mutations and their role in the pathogenesis of glioma can be also evaluated.

Materials and methods

C6 cell culture and isolation of C6 ρ 0 clone cell line. The rat C6 glioma cell line was purchased from the Institute of Culture Collection of the Chinese Academy of Sciences and cultured in F-12 Ham medium (Gibco; Thermo Fisher Scientific, Inc.) supplemented with 2% fetal bovine serum (Zhejiang Tianhang Biotechnology Co., Ltd.), 15% horse serum (Tianjin Kangyuan Biotechnology Co., Ltd.) and 1% penicillin (100 U/ml) and streptomycin (100 μ g/ml; both from Corning, Inc.). The medium was changed every three days and sub-cultures were made when the cells reached 80% confluence. The cells were maintained at 37°C, 5% CO₂ and 90% humidity.

The generation of C6 ρ 0 cells was performed by exposing wild-type C6 glioma cells to 5 μ M EB and 8 μ M ddC in F-12 Ham medium supplemented with uridine (50 μ g/ml) and pyruvate (0.1 mg/ml), with a daily change of the culture medium. Cells (2x10⁶) were incubated in the above medium at 37°C, 5% CO₂ and 90% humidity and the expression of mtDNA was measured using a mtDNA-specific PCR for a set period of time until mtDNA band completely disappeared.

Single cell clones were isolated and collected by the limiting dilution method (16) when the mtDNA band disappeared. When no mtDNA fragment was detected by PCR, the treated cells were quickly plated into 96-well plates at a density of one cell per well to isolate pure cell clones derived from the heterogeneous colony. Screening and isolation of C6 ρ 0 cells were performed as shown in Fig. 1.

A single colony in 96-well was observed under an inverted phase contrast microscope (Olympus Corporation); a single C6 ρ 0 cell was marked and the wells containing >2 cells were discarded. When the single colony was spread in the 96-well plate, it was transferred into 48, 24, 12 and 6-well plates one after the other after spreading the cells in each of them to gradually expand the cell amount. To verify the absence of mtDNA, each potential C6 ρ 0 cell line was divided into two halves: One half was used to study the survival ability in pyrimidines and pyruvate-absent C6 ρ 0 test medium and the other half was cultured in F-12 Ham medium containing uridine (50 μ g/ml) and pyruvate (0.1 mg/ml). Trypan blue at a dose of 0.2% was used to test and count the viable cells. Finally, the C6 ρ 0 characteristic in these isolated colonies was confirmed by mtDNA-specific PCR.

To evaluate cell growth, C6 and C6 ρ 0 cells were plated in triplicate and the number of cells were counted on five consecutive days. In order to standardize the condition of the cell culture, C6 and C6 ρ 0 cells were cultured in F-12 Ham medium supplemented with 50 μ g/ml uridine and 0.1 mg/ml pyruvate to evaluate the growth characteristics.

Production of transmitochondrial cybrids. The fusion between C6 ρ 0 and rat blood platelets was performed using the approach of standard chemical enucleation/polyethylene

glycol fusion (18). The fusion cells were placed on a test bench for 1 min at 25°C and diluted with a mixture (10 ml) of F-12 Ham and FBS (10%) supplemented with uridine (50 μ g/ml) and pyruvate (0.1 mg/ml) and the suspension was placed into petri dishes (5 dishes, 2x10⁵ cells/dish). The medium was replaced with the selective medium (without pyruvate and uridine) after 3 days.

PCR analysis of mtDNA. In order to detect mtDNA in C6, C6 ρ 0 and cybrids, total DNA from a different number of cells was isolated as a template using a commercial kit (Tiangen Biotech Co., Ltd.), following the manufacturer's instructions. Oligonucleotide primers were used to amplify the nucleotide sequences of rat mtDNA mitochondrial D-loop region. The primers were synthesized by Sangon Biotech Co., Ltd. mtDNA was amplified using a volume of 50 μ l containing 0.25 μ l units of TakaRa Ex Taq polymerase (Takara Biotechnology Co., Ltd.) and 0.2 μ l primer pair. Primers specific for the mtDNA D-loop region were the following: Forward 5'-CCTCCATT CATTATCGCCGCCCTTGC-3' and reverse 5'-GTCTGG GTCTCCTAGTAGGTCTGGGAA-3' (235 bp). The PCR conditions were: 35 cycles of denaturation at 98°C for 10 sec, annealing at 60°C for 30 sec and extension at 72°C for 60 sec. The products were separated by 1% agarose gel electrophoresis and images were detected using a 5200 Multi Luminescent image analyzer, according to the manufacturer's protocol (Tanon Science and Technology Co., Ltd.). The intensity of the bands indicated the amount of mtDNA.

Transmission electron microscopy (TEM). Cells for TEM were collected and plated on coverglasses according to the method of Kukat *et al* (20). Cells grown on cover slips were fixed with a solution of 2.5% glutaraldehyde in 100 mM cacodylate buffer, pH 7.4 for 1.5 h at 4°C, washed twice with cacodylate buffer, followed by a fixation with 2% osmium tetroxide in 50 mM cacodylate buffer (pH 7.4). Specimens were washed twice with distilled water and stained over night with aqueous 0.5% uranyl acetate at 4°C. Cells were dehydrated, embedded in Epon 812 and sectioned at 60 nm. Mitochondrial morphology was observed using a H7000 electron microscope at 80 kV (Hitachi, Ltd.). Negatives were digitized by scanning and processed with Adobe Photoshop CC (Adobe Systems, Inc.).

Mitochondrial mass change and sugar uptake. Cells (2x10⁶ cells) were plated in 35 mm dishes for 24 h and incubated with 100 nM Mito-Tracker Green (Thermo Fisher Scientific, Inc.) or 10 μ M 2-NBDG, a fluorescent glucose, for 30 min at 37°C in the dark, to analyze the mitochondrial mass and sugar intake. Cells were detached by trypsin, collected, resuspended in saline solution and analyzed by flow cytometry. In each measurement, fluorescence intensity data from 2x10⁴ single cell events were collected by an ACEA NovoCyte2040R flow cytometer (ACEA Bioscience, Inc.; Agilent Technologies, Inc.), using fluorescence excitation/emission (Ex/Em) wavelengths of 490/516 nm to evaluate the mitochondrial mass and Ex/Em of 480/525 nm to evaluate cell sugar uptake.

ATP consumption by C6 and C6 ρ 0. An enhanced ATP Assay kit (Beyotime Institute of Biotechnology) was used to evaluate cellular ATP levels following the manufacturer's

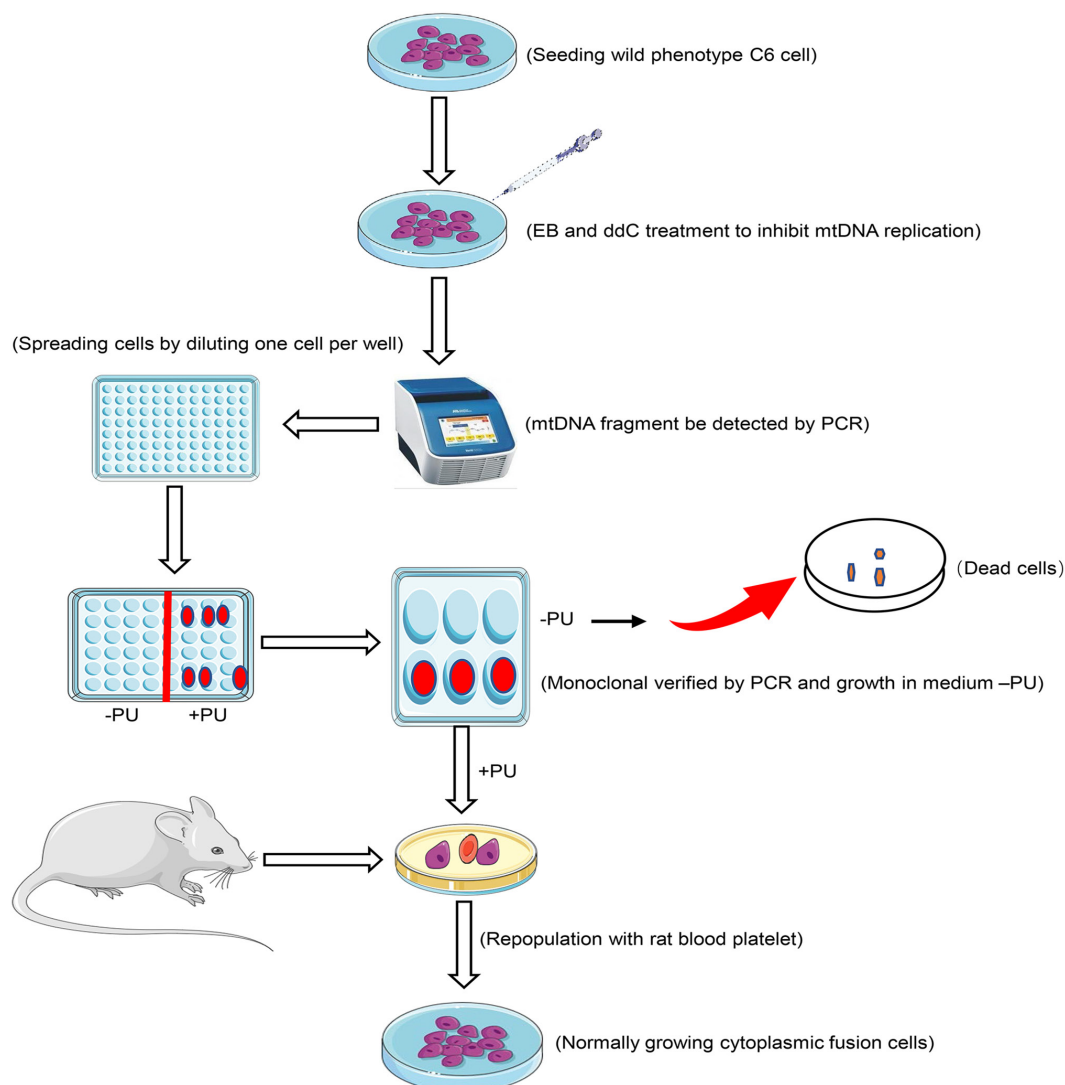


Figure 1. Schematic diagram of the protocol used to isolate the target cells and to generate fusion cells. EB, ethidium bromide; ddC, 2',3'-dideoxycytidine; mtDNA, mitochondrial DNA; -PU, growth in a medium without pyruvate and uridine; +PU, growth in a medium supplemented with pyruvate and uridine.

instructions. The cell lysates were centrifuged ($12,000 \times g$ at 4°C for 5 min) and the supernatant was collected and transferred into a 96-well plate containing the detection solution. The samples were then incubated for 30 min at 37°C and the luminescence signal was detected. Total ATP levels were calculated from the relationship between luminescence signals and protein concentration.

Detection of cellular reactive oxygen species (ROS) production. Cells were plated in 35 mm dishes (2×10^6 cells) for 24 h and incubated with 2,7-dichlorodihydrofluorescein diacetate (DCFH-DA; $10 \mu\text{M}$; Sigma-Aldrich; Merck KGaA) or $5 \mu\text{M}$ MitoSOX Red (Thermo Fisher Scientific, Inc.) for 30 min at 37°C in the dark to analyze total ROS and mitochondrial ROS, respectively. Cells were detached by trypsin, collected, resuspended in saline solution and analyzed by a NovoCyte 2040R (ACEA Biosciences Inc.) flow cytometer. Ex/Em of 480/525 was set for the evaluation of total ROS, while Ex/Em of 510/580 was set for the evaluation of mitochondrial ROS. The amount of ROS produced was expressed as fluorescence intensity relative to the one of untreated cells.

Determination of mitochondrial membrane potential ($\Delta\Psi\text{m}$). Cells were plated in dishes (2×10^6 cells) containing F-12 Ham medium for 24 h prior to the detection of $\Delta\Psi\text{m}$. The cells were then collected, washed and resuspended in phosphate-buffered saline. Finally, $10 \mu\text{M}$ JC-1 (Beijing Solarbio Science & Technology Co., Ltd.) stain was added into the buffer and carbonyl cyanide m-chlorophenylzone, a potent mitochondrial membrane disruptor, was used as the positive control. The cells were incubated for 30 min (37°C ; $5\% \text{CO}_2$) and then fluorescence intensity of 1×10^5 single cell events was processed by a NovoCyte 2040R flow cytometer (ACEA Biosciences Inc.) according to the manufacturer's protocol. Ex/Em of 490/530 and Ex/Em of 525/590 was used for ratio analysis. The ratio of red/green (PE/FITC) fluorescence intensity was used to determine $\Delta\Psi\text{m}$.

Statistical analysis. Statistical analysis was performed using GraphPad Prism software (version 6; GraphPad Software, Inc.). Results were presented as means \pm standard deviation ($n=3$). Comparisons among multiple groups were analyzed using one-way ANOVA followed by Bonferroni's post hoc test.

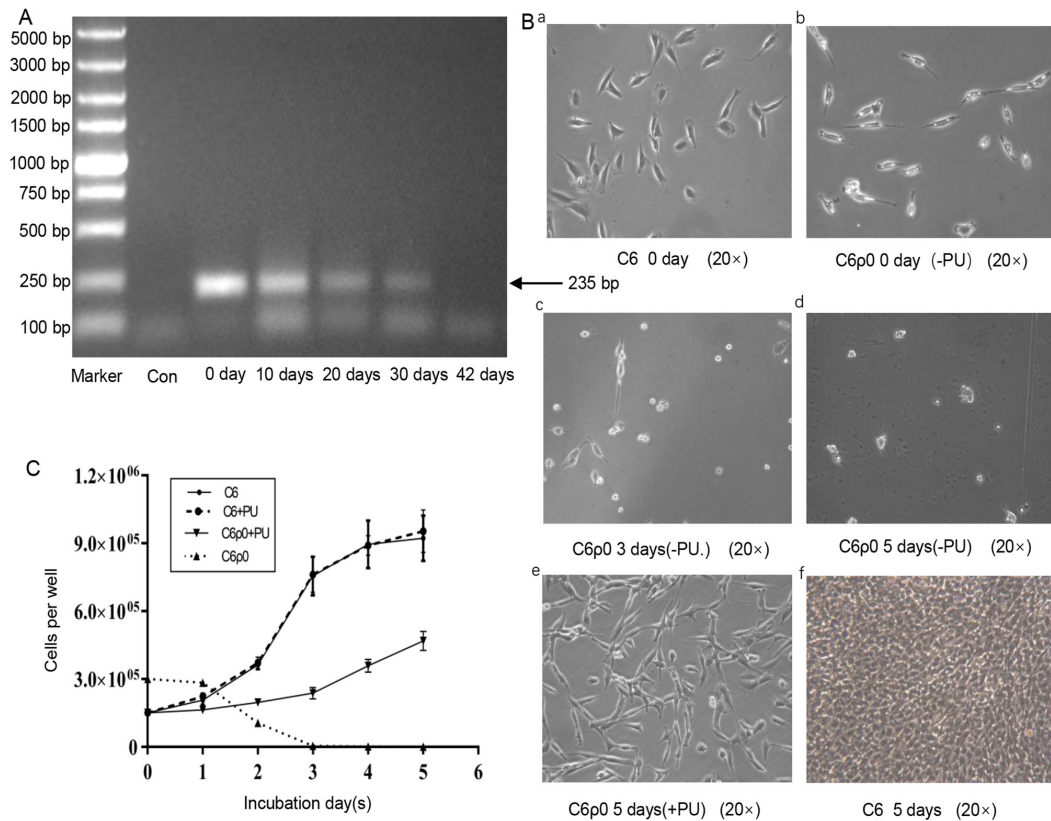


Figure 2. Establishment of C6p0 cells and growth characteristic of C6 and C6p0 cells in different media. (A) Cells were treated with EB (5 μ M) and ddC (8 μ M) for 6 weeks. The same amount of C6 cells (4×10^5) was used in the different groups. The content of mtDNA was determined by an mtDNA-specific PCR. The PCR products were visualized on 1% agarose gel by EB staining. Marker: 5000 DNA ladder. (B) Representative images of C6 and C6p0 clone cells growing in different media and at a different time points. (B-a and f) C6 cells were cultured in F-12 medium at day 0 and day 5, respectively. (B-b, c and d) C6p0 cells cultured in F-12 (-PU) at day 0, day 3 and day 5, respectively. (B-e) C6p0 cells cultured in F-12 (+PU) medium at day 5. (C) C6 and C6p0 were cultured in media with or without pyruvate and uridine for 5 days and cell proliferation was measured and compared. After seeding (0 d) and growing for 5 days in various media, the number of cells per well was counted. EB, ethidium bromide; ddC, 2',3'-dideoxycytidine; mtDNA, mitochondrial DNA; Con, sample without template; -PU, growth in a medium without pyruvate and uridine; +PU, growth in a medium supplemented with pyruvate and uridine.

Comparisons between two groups were analyzed using unpaired Student's t-test. $P < 0.05$ was considered to indicate a statistically significant difference.

Results

Effect of EB and ddC treatment on mtDNA content. The mtDNA content decreased with the increase of the treatment time (Fig. 2A). After 6 weeks exposure, the amplification of mtDNA-encoded D-loop region gene was lost in C6p0 cells (42 days), while the parental C6 cells (0 day) yielded strong PCR products at the predicted size. Taken together, the results suggested that mtDNA was specifically depleted from C6 cells and that C6p0 cells survived in the culture supplemented with uridine and pyrimidine.

Fig. 2B-a and B-b demonstrated that the single colony of C6p0 and its parent cells were morphologically slightly different. To verify the C6p0 stage of the cloned cells, the growth of C6p0 cells was analyzed in the medium without uridine and pyruvate. As shown in Fig. 2B-c and B-d, the number of C6p0 cells became fewer, as they were no longer able to grow in ordinary medium, until their total disappearance. All cells could survive for several days, but at day 5, no living C6p0 cells were identified by the trypan blue exclusion method (Fig. 2B-d). By contrast, C6p0 cells cultured in uridine and

pyruvate and C6 cells cultured in selective medium grew vigorously and quickly (Fig. 2B-e), thus demonstrating that the presence or absence of uridine and pyrimidine had no effect on C6 cell growth, while their presence was essential for the growth of C6p0 cells (Fig. 2C).

Repopulation with exogenous mitochondria from rat platelets. Rat platelets were used as exogenous mitochondrial donors to perform repopulation experiments on the C6p0 clone (Fig. 3A). The cybrid cells were analyzed to verify the presence of mtDNA using the mtDNA-specific PCR. As shown in Fig 3B, PCR bands corresponding to mtDNA appeared in both cybrid and wild type C6 cells, suggesting the retention of mtDNA in cybrid cells.

The morphology of mitochondria was significantly different in C6 and C6p0 cells. Wild-type C6 and cybrid cells displayed a typical mitochondrial morphology, with organized cristae, electron-dense matrix and intact mitochondrial membrane (Fig. 3C-a and C-c), while mitochondria in C6p0 cells were irregularly expanded, with a partial or almost complete dissolution of the internal cristae (Fig. 3C-b). When the cloned C6p0 cells were fused with rat platelets, the cybrid cells grew well in selective medium without pyruvate and uridine and thus, the repopulated colonies were formed, as shown in Fig. 3D.

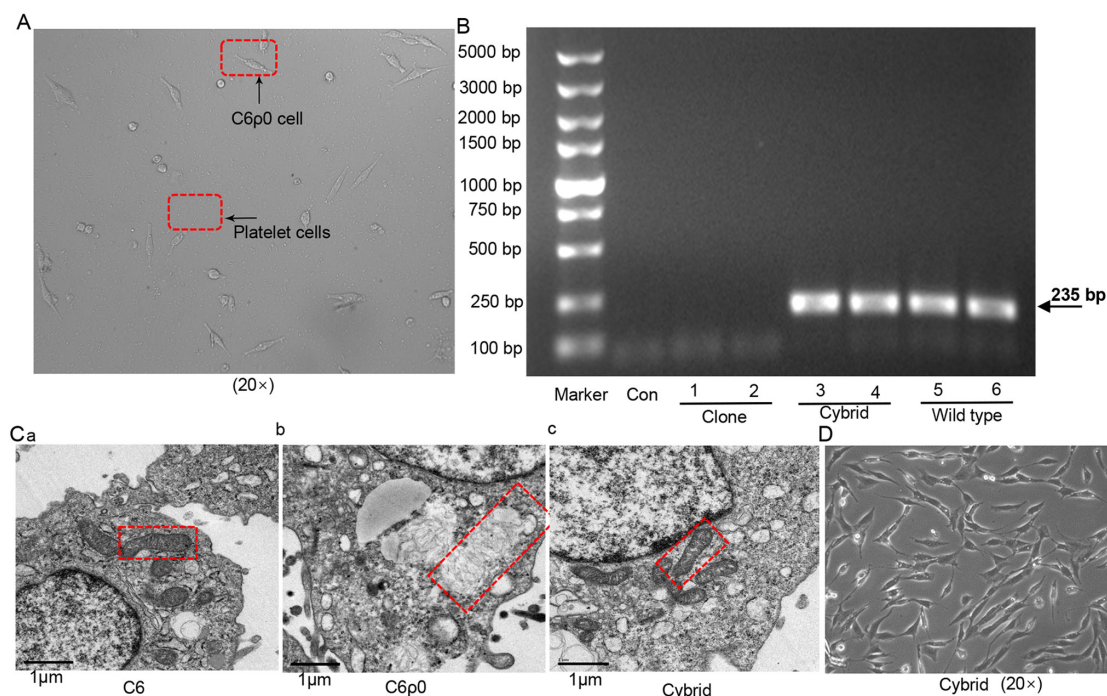


Figure 3. Construction and identification of cytoplasmic hybrid cells. (A) C6p0 clone fusion with rat platelets: Cybrid cells derived from the fusion between C6p0 clone and platelets isolated from rat blood samples. (B) Presence of mtDNA in cybrid cells and wild-type cells evaluated by mtDNA-specific PCR after 10 days of culture. Two different amounts of cells (2×10^5 cells in 1, 3, 5 lane and 4×10^5 cells in 2, 4, 6 lane) were used in this experiment. The PCR products were visualized on 1% agarose gel by EB staining. Marker, 5000 DNA ladder. (C) TEM images of (a) C6, (b) C6p0 and (c) cybrid cells (mitochondria indicated by red box), magnification $\times 25,000$ in all cells. (D) Representative image of cybrid cells growing normally in media without pyruvate and uridine. mtDNA, mitochondrial DNA; EB, ethidium bromide; Con, sample without template; Clone, monoclonal C6p0; Cybrid, C6p0 cell fused with rat blood platelets; Wild type, C6 cells.

Mitochondrial mass change and sugar uptake in C6 and C6p0. C6p0 cells were characterized by a notable and significant decrease in mitochondrial mass, compared with that in C6 cells ($P < 0.001$; Fig. 4A).

To verify whether the decreased mitochondrial mass had an effect on sugar uptake, the C6 and C6p0 cells were exposed to $10 \mu\text{M}$ 2-NBDG for 30 min and the sugar content in the cells was evaluated by flow cytometry. Quantitative analysis results showed no difference in sugar uptake between C6 and C6p0 cells (Fig. 4B). However, the ATP assay showed that C6p0 consumed less ATP compared with C6 cells (Fig. 4C).

ROS changes in C6 and C6p0 cells. The amount of total ROS production was significantly reduced in C6p0 cells compared with its production in wild type C6 (Fig. 4D). To evaluate whether this was due to the difference in mitochondria between the two cell types, the source of ROS was identified. The results showed that C6 cells produced more mitochondrial ROS than C6p0 cells. Some chemicals targeting mitochondria can stimulate C6 cells to produce more mitochondrial-derived ROS; for instance, rotenone and EB treatment can produce a large amount of mitochondrial ROS in C6 compared with in C6p0 (Fig. 4E). This result confirmed that the change in ROS amount between C6 and C6p0 cells was mainly due to the difference in mitochondria; the existence and integrity of mtDNA has a great influence on the production of ROS

Flow cytometric analysis of $\Delta\Psi\text{m}$ in C6 and C6p0 cells. To determine the $\Delta\Psi\text{m}$ changes in mtDNA depleted cells, cells

were stained with JC-1 and the results of flow cytometry showed a distinct decline in $\Delta\Psi\text{m}$ from untreated C6 cells, 2-day EB-treated C6 cells and C6p0 monoclonal cells (Fig. 5). These results suggested that the treatment with EB induced a significant decrease in $\Delta\Psi\text{m}$. Thus, the $\Delta\Psi\text{m}$ detected in C6p0 cells was reduced by two-thirds compared with C6 cells.

Discussion

Mitochondria are the main source of cellular energy and serve a role in cell proliferation, growth and differentiation through continuous fusion and division (21). The mitochondrial genome is essential for a normal cellular function and it encodes important subunits of the mitochondrial respiratory chain and F₀F₁-ATPase, which are required for oxidative phosphorylation. Depletion of mtDNA results in the inhibition of the mitochondrial respiratory chain and the loss of mtDNA-encoded mitochondrial enzyme activity (16,22-24).

In the present study, persistent mtDNA damage of C6 cells by EB and ddC successfully induced the C6p0 cell phenotype. EB is known for its insertion in mammalian mtDNA, thus inhibiting mtDNA replication (25,26), and ddC is used as an antiretroviral drug that can reduce the level of mtDNA by inhibiting mitochondrial DNA polymerase γ (27). Therefore, these two compounds have the ability to reduce the amount of mtDNA by interfering with mtDNA replication or inhibiting polymerase γ .

Indeed, in the present study C6p0 monoclonal cells were successfully obtained through the treatment with the mixture

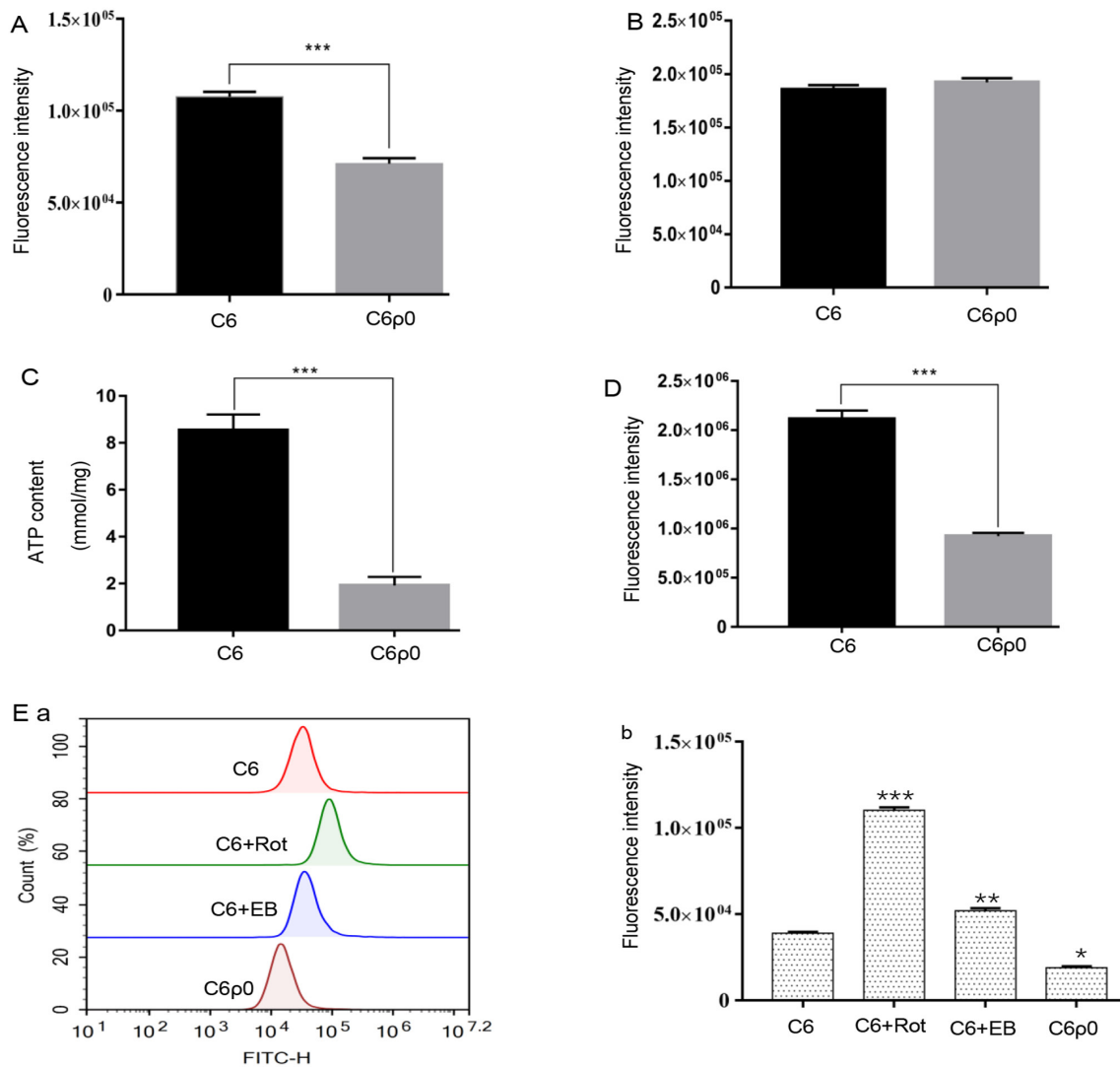


Figure 4. Characteristics of the generated C6 ρ 0 and C6 cells. (A) Mitochondrial mass detected by flow cytometry. (B) Quantification of the sugar uptake by flow cytometry. (C) ATP consumption in C6 and C6 ρ 0 cells. (D) Accumulation of total ROS in C6 and C6 ρ 0 cells. (E) Accumulation of mitochondrial ROS in C6 and C6 ρ 0 cells. (E-a) Mitochondrial ROS were detected by flow cytometer. (E-b) Fluorescence intensity data were expressed as mean \pm SD. Quantification of the fluorescence intensity; *** P <0.001, ** P <0.01 and * P <0.05 vs. the C6 group. Comparisons between two groups were analyzed using unpaired Student's *t*-test and multiple groups were analyzed using one-way ANOVA. P <0.05 was considered to indicate a statistically significant difference. Results are shown as mean \pm standard deviation from three independent experiments. Rot, rotenone; EB, ethidium bromide.

of EB and ddC as reported by the literature. As a result, enzymes involved in pyrimidine biosynthesis cannot be activated, resulting in the inability of C6 ρ 0 cells to remain alive without uridine and pyruvate (28). The morphology of mitochondria in C6 and C6 ρ 0 cells observed by TEM revealed the presence of elongated mitochondria with parallel and normal electron density in the wild-type cells, while disordered swollen mitochondria were found in C6 ρ 0 cells. The changes in C6 ρ 0 cells were due to the loss of the mitochondrial genome and in agreement with the results of previous studies (17,20,29).

However, not all cell types treated with EB and ddC can result in pure ρ 0 cells. Indeed, in the present study HepG2 and Huh7 cells did not lose all their mtDNA following the above treatment (data not shown). This is because not all cells are sensitive to drugs that destroy mtDNA. Thus far, only several cell types can form pure ρ 0 cells that can be used for further research (17,20,26,30).

Since mtDNA-depleted cells provide a cytoplasmic hybrid model for studying mtDNA single nucleotide polymorphisms with the same nuclear DNA background, they are considered an effective tool for studying mitochondrial disorders (15). mtDNA and nuclear DNA can control mitochondrial functions and the cybrids allow researchers to evaluate whether the mtDNA or nuclear DNA function is involved in a mitochondrial defect (31). In the present study, a practical and reliable technique was developed to produce C6 ρ 0 monoclonal cells and cybrids generated with rat platelets. The experiments on the growth characteristics of C6 and C6 ρ 0 cells showed that the growth rate of C6 ρ 0 was significantly reduced compared with the parental cells and that uridine and pyruvate were necessary for their growth. Nevertheless, cybrids grew as much as the wild-type cells and did not need the help of uridine and pyruvate. However, it has been reported that the T47D ρ 0, MOLT-4 ρ 0, HeLa ρ 0, 143BTK ρ 0 cells grow slower than their parent cells (17,20,29,32). It is

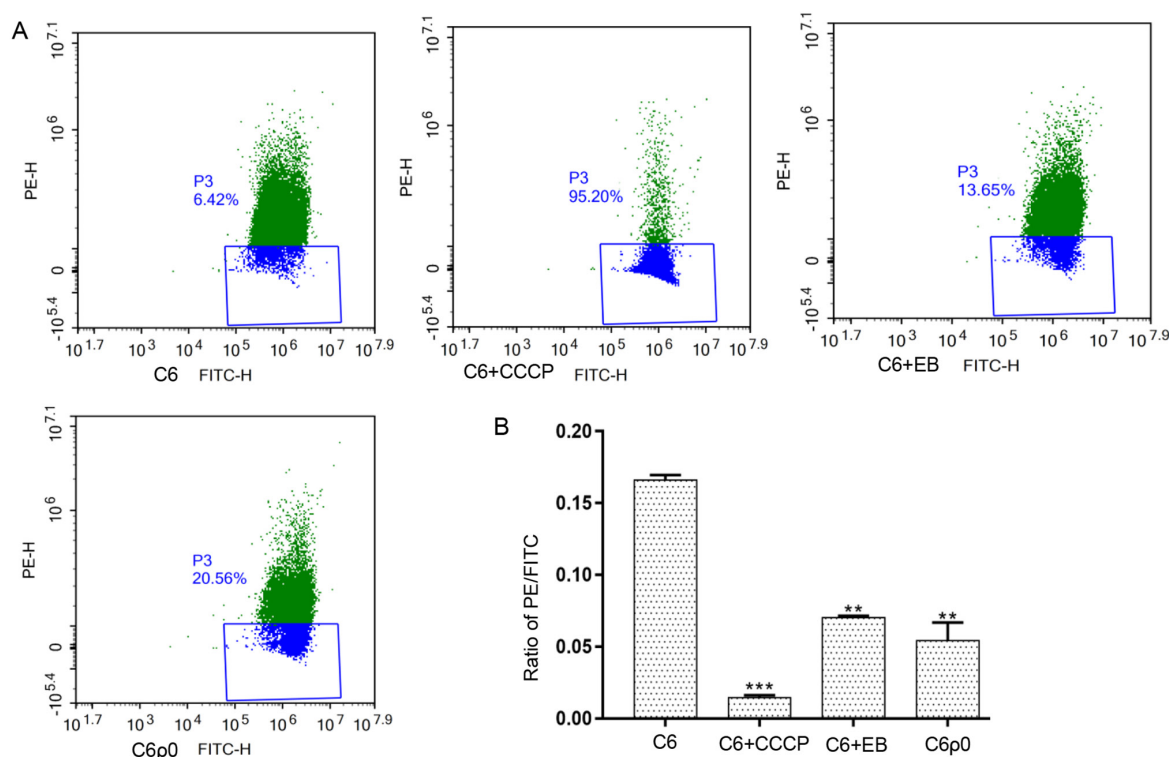


Figure 5. Comparative study of C6 and C6p0 mitochondrial membrane potential. (A) Flow cytometry analysis of $\Delta\Psi_m$ in C6 and C6p0 cells. (B) Quantification of the fluorescence intensity; *** $P < 0.001$ and ** $P < 0.01$ vs. the C6 group (one-way ANOVA). Results are shown as mean \pm standard deviation from three independent experiments. C6, wild-type cells; C6+CCCp, C6 cells treated with a membrane potential positive agent; C6+EB, C6 cells treated with EB for 2 days. C6p0, C6p0 monoclonal cells; CCCp, carbonyl cyanide *m*-chlorophenzone.

noteworthy that the hepatoma Hepall-6p0 and HepG2p0 cells proliferate several times more than the wild-type cells, suggesting that different types of cells may exhibit different sensitivities to the intracellular changes caused by mtDNA and not all cell types proliferate less after mtDNA depletion (33).

The number of mitochondria is closely associated with the energy cell metabolism (34). In the present study, the mitochondrial mass of C6p0 cells was notably decreased compared with the mitochondrial mass in C6 cells. The hypothesis was that the decrease of mtDNA content in C6p0 cells led to mitochondrial dysfunction and that changes in energy metabolism and ATP content may destroy unconstrained tumor cell proliferation and invasion (35). A series of cellular changes and diseases are closely associated with mtDNA mutations (36). By contrast, some studies have identified that the increasing mtDNA content is a self-protection mechanism that prevents apoptosis and increases tumor cell sensitivity to chemotherapeutic drugs (37,38). The mitochondrial content in the cell determines the apoptotic fate and modulates the time of death, since cells with higher mitochondrial content are more prone to die (39). In fact, the amount of all apoptotic proteins is modulated by the mitochondrial content (40). It is also hypothesized that mtDNA destruction can enhance the apoptosis of certain cells *in vivo* and inhibit the tumorigenicity of certain tumor cells (41).

Mitochondria are the major source of ROS, which serve key roles in both physiological and pathological processes and act as mediators in a number of cellular signaling pathways in the cell (42). An increase in ROS levels can trigger a protective response by activating antioxidant

response elements (43). However, the increase of ROS damages proteins, fats and nucleic acids, triggering other stress responses or cell death (44,45). Conversely, appropriate levels of ROS can reduce cancer, diabetes and delay aging (46). In the present study, the increase in ROS content of rotenone-treated C6 cells was more than twice that of non-treated C6 cells, while ROS levels in monoclonal C6p0 clearly decreased. These results demonstrated that drugs targeting the complex I, III and V of the respiratory chain (11,47) can cause the increase of ROS, but they have a weak effect on mitochondrial DNA depleted cells.

Mitochondria are key regulators of cell death through alterations in the $\Delta\Psi_m$ to respond to various unfavorable situations. The results of the present study showed that the $\Delta\Psi_m$ in C6 cells was reduced following EB treatment, while the reduction of $\Delta\Psi_m$ in C6p0 cells was one third of that of the parent cells. In addition, the C6p0 cells remained alive at relatively low $\Delta\Psi_m$. These results indicated that the complete depletion of the mtDNA in C6p0 cells was not associated to a complete disappearance of the $\Delta\Psi_m$. Some studies have demonstrated that mitochondria with a dysfunctional respiratory chain can still generate $\Delta\Psi_m$ by the use of glycolytic ATP (18,48). A previous study suggested that the change in the membrane status leads to changes in external oxidative stress tolerance and has an influence on the efficacy of cancer therapy (32).

Overall, the method of the present study proved efficient and reliable; the defects in the mitochondrial structure and function in C6p0 cells can lead to impairments in cell proliferation *in vitro*. Therefore, C6p0 cell lines with different

nuclear backgrounds could be used as a model in future experiments to study glioma associated with mitochondria.

Acknowledgements

Not applicable.

Funding

The present study was supported by grants from the National Science Foundation of China (grant no. 31870333), Qinghai Provincial Science Foundation (grant no. 2019-ZJ-7023), Qinghai Province International Cooperation Project (grant no. 2018-HZ-812), the Taishan Scholar Program of Shandong Province (grant no. tshw201502046) and the Shuangbai Project of Yantai and Youth Innovation Promotion Association, CAS.

Availability of data and materials

The datasets used and/or analyzed in the current study are available from the corresponding author upon reasonable request.

Authors' contributions

HW and ZW conceived the study. JL and BB designed the experiments. YJ and GL performed the experiments. YJ and GL analyzed the data. YJ wrote the manuscript. All authors read and approved the final manuscript.

Ethics approval and consent to participate

Not applicable.

Patient consent for publication

Not applicable.

Competing interests

The authors declare that they have no competing interests.

References

- Ostrom QT, Gittleman H, Fulop J, Liu M, Blanda R, Kromer C, Wolinsky Y, Kruchko C and Barnholtz-Sloan JS: CBTRUS statistical report: Primary brain and central nervous system tumors diagnosed in the united states in 2008-2012. *Neuro Oncol* 17 (Suppl 4): iv1-iv62, 2015.
- Liu CA, Chang CY, Hsueh KW, Su HL, Chiou TW, Lin SZ and Harn HJ: Migration/invasion of malignant gliomas and implications for therapeutic treatment. *Int J Mol Sci* 19: 1115, 2018.
- Chatterjee A, Mambo E and Sidransky D: Mitochondrial DNA mutations in human cancer. *Oncogene* 25: 4663-4674, 2006.
- Rocha EM, De Miranda B and Sanders LH: Alpha-synuclein: Pathology, mitochondrial dysfunction and neuroinflammation in Parkinson's disease. *Neurobiol Dis* 109: 249-257, 2018.
- Verma P, Singh A, Nthenge-Ngumbau DN, Rajamma U, Sinha S, Mukhopadhyay K and Mohanakumar KP: Attention deficit-hyperactivity disorder suffers from mitochondrial dysfunction. *BBA Clin* 6: 153-158, 2016.
- Kraya T, Deschauer M, Joshi PR, Zierz S and Gaul C: Prevalence of headache in patients with mitochondrial disease: A cross-sectional study. *Headache* 58: 45-52, 2018.
- Szendroedi J, Phielix E and Roden M: The role of mitochondria in insulin resistance and type 2 diabetes mellitus. *Nat Rev Endocrinol* 8: 92-103, 2011.
- Theurey P and Pizzo P: The aging mitochondria. *Genes (Basel)* 9: 22, 2018.
- Schapira AH: Mitochondrial disease. *Lancet* 368: 70-82, 2006.
- Sharma P and Sampath H: Mitochondrial DNA integrity: Role in health and disease. *Cells* 8: 100, 2019.
- Dias N and Bailly C: Drugs targeting mitochondrial functions to control tumor cell growth. *Biochem Pharmacol* 70: 1-12, 2005.
- Govindaraj P, Rani B, Sundaravadivel P, Vanniarajan A, Indumathi KP, Khan NA, Dhandapany PS, Rani DS, Tamang R, Bahl A, *et al*: Mitochondrial genome variations in idiopathic dilated cardiomyopathy. *Mitochondrion* 48: 51-59, 2019.
- Spadafora D, Kozhukhar N, Chouljenko VN, Kousoulas KG and Alexeyev MF: Methods for efficient elimination of mitochondrial DNA from cultured cells. *PLoS One* 11: e0154684, 2016.
- Yang L, Long Q, Liu J, Tang H, Li Y, Bao F, Qin D, Pei D and Liu X: Mitochondrial fusion provides an 'initial metabolic complementation' controlled by mtDNA. *Cell Mol Life Sci* 72: 2585-2598, 2015.
- Chomyn A: Platelet-mediated transformation of human mitochondrial DNA-less cells. *Methods Enzymol* 264: 334-339, 1996.
- Yoon YG, Oh YJ and Yoo YH: Rapid isolation of mitochondrial DNA-depleted mammalian cells by ethidium bromide and dideoxycytidine treatments. *J App Biol Chem* 57: 259-265, 2014.
- Yu M, Shi Y, Wei X, Yang Y, Zhou Y, Hao X, Zhang N and Niu R: Depletion of mitochondrial DNA by ethidium bromide treatment inhibits the proliferation and tumorigenesis of T47D human breast cancer cells. *Toxicol Lett* 170: 83-93, 2007.
- Fernández-Moreno M, Hermida-Gómez T, Gallardo ME, Dalmao-Fernández A, Rego-Pérez I, Garesse R and Blanco FJ: Generating rho-0 cells using mesenchymal stem cell lines. *PLoS One* 11: e0164199, 2016.
- Binder DR, Dunn WH Jr and Swerdlow RH: Molecular characterization of mtDNA depleted and repleted NT2 cell lines. *Mitochondrion* 5: 255-265, 2005.
- Kukat A, Kukat C, Brocher J, Schäfer I, Krohne G, Trounce IA, Villani G and Seibel P: Generation of rho0 cells utilizing a mitochondrially targeted restriction endonuclease and comparative analyses. *Nucleic Acids Res* 36: e44, 2008.
- Holmuhamedova E, Jahangira A, Bienengraeber M, Lewis LD and Terzic A: Deletion of mtDNA disrupts mitochondrial function and structure, but not biogenesis. *Mitochondrion* 3: 13-19, 2003.
- Alston CL, Rocha MC, Lax NZ, Turnbull DM and Taylor RW: The genetics and pathology of mitochondrial disease. *J Pathol* 241: 236-250, 2017.
- Meiliana A, Dewi NM and Wijaya A: Mitochondria in health and disease. *Indonesian Biomedical J* 11: 1-15, 2019.
- Miller SW, Trimmer PA, Davis Parker W Jr and Davis RE: Creation and characterization of mitochondrial DNA-depleted cell lines with 'neuronal-like' properties. *J Neurochem* 67: 1897-1907, 1996.
- Desjardins P, Frost E and Morais R: Ethidium bromide-induced loss of mitochondrial DNA from primary chicken embryo fibroblasts. *Mol Cell Biol* 5: 1163-1169, 1985.
- Armand R, Channon JY, Kintner J, White KA, Miselis KA, Perez RP and Lewis LD: The effects of ethidium bromide induced loss of mitochondrial DNA on mitochondrial phenotype and ultrastructure in a human leukemia T-cell line (MOLT-4 cells). *Toxicol Appl Pharmacol* 196: 68-79, 2004.
- Nelson I, Hanna MG, Wood NW and Harding AE: Depletion of mitochondrial DNA by ddC in untransformed human cell lines. *Somat Cell Mol Genet* 23: 287-290, 1997.
- King MP and Attardi G: Isolation of human cell lines lacking mitochondrial DNA. *Methods Enzymol* 264: 304-313, 1996.
- Wochna A, Niemczyk E, Kurono C, Masaoka M, Majczak A, Kedzior J, Slominska E, Lipinski M and Wakabayashi T: Role of mitochondria in the switch mechanism of the cell death mode from apoptosis to necrosis-studies on rho0 cells. *J Electron Microsc* (Tokyo) 54: 127-138, 2005.
- Schauen M, Spitkovsky D, Schubert J, Fischer JH, Hayashi J and Wiesner RJ: Respiratory chain deficiency slows down cell-cycle progression via reduced ROS generation and is associated with a reduction of p21CIP1/WAF1. *J Cell Physiol* 209: 103-112, 2006.
- Inoue K, Takai D, Hosaka H, Ito S, Shitara H, Isobe K, LePecq JB, Segal-Bendirdjian E and Hayashi J: Isolation and characterization of mitochondrial DNA-less lines from various mammalian cell lines by application of an anticancer drug, ditercalinium. *Biochem Biophys Res Commun* 239: 257-260, 1997.

32. Tomita K, Kuwahara Y, Takashi Y, Tsukahara T, Kurimasa A, Fukumoto M, Nishitani Y and Sato T: Sensitivity of mitochondrial DNA depleted ρ^0 cells to H_2O_2 depends on the plasma membrane status. *Biochem Biophys Res Commun* 490: 330-335, 2017.
33. Boland ML, Chourasia AH and Macleod KF: Mitochondrial dysfunction in cancer. *Front Oncol* 3: 292, 2013.
34. Vyas S, Zaganjor E and Haigis MC: Mitochondria and Cancer. *Cell* 166: 555-566, 2016.
35. Penrose HM, Heller S, Cable C, Nakhoul H, Ungerleider N, Baddoo M, Pursell ZF, Flemington EK, Crawford SE and Savkovic SD: In colonic ρ^0 (rho0) cells reduced mitochondrial function. *Oncoscience* 4: 189-198, 2017.
36. Pessôa LVF, Bressan FF, Chiaratti MR, Pires PR, Perecin F, Smith LC and Meirelles FV: Mitochondrial DNA dynamics during in vitro culture and pluripotency induction of a bovine Rho0 cell line. *Genet Mol Res* 14: 14093-14104, 2015.
37. Mei H, Sun S, Bai Y, Chen Y, Chai R and Li H: Reduced mtDNA copy number increases the sensitivity of tumor cells to chemotherapeutic drugs. *Cell Death Dis* 6: e1710, 2015.
38. Zong WX, Rabinowitz JD and White E: Mitochondria and cancer. *Mol Cell* 61: 667-676, 2016.
39. Grady JP, Pickett SJ, Ng YS, Alston CL, Blakely EL, Hardy SA, Feeney CL, Bright AA, Schaefer AM, Gorman GS, *et al*: mtDNA heteroplasmy level and copy number indicate disease burden in m.3243A>G mitochondrial disease. *EMBO Mol Med* 10: e8262, 2018.
40. Márquez-Jurado S, Díaz-Colunga J, das Neves RP, Martínez-Lorente A, Almazán F, Guantes R and Iborra FJ: Mitochondrial levels determine variability in cell death by modulating apoptotic gene expression. *Nat Commun* 9: 389, 2018.
41. Papal S and Skulachev VP: Reactive oxygen species, mitochondria, apoptosis and aging. *Mol Cell Biochem* 174: 305-319, 1997.
42. Frazier AE, Thorburn DR and Compton AG: Mitochondrial energy generation disorders: Genes, mechanisms, and clues to pathology. *J Biol Chem* 294: 5386-5395, 2019.
43. Shadel GS and Horvath TL: Mitochondrial ROS signaling in organismal homeostasis. *Cell* 163: 560-569, 2015.
44. Nunnari J and Suomalainen A: Mitochondria: In sickness and in health. *Cell* 148: 1145-1159, 2012.
45. Meyer JN, Hartman JH and Mello DF: Mitochondrial toxicity. *Toxicol Sci* 162: 15-23, 2018.
46. Ristow M, Zarse K, Oberbach A, Klötting N, Birringer M, Kiehntopf M, Stumvoll M, Kahn CR and Blüher M: Antioxidants prevent health-promoting effects of physical exercise in humans. *Proc Natl Acad Sci USA* 106: 8665-8670, 2009.
47. Zorov DB, Juhaszova M and Sollott SJ: Mitochondrial reactive oxygen species (ROS) and ROS-induced ROS release. *Physiol Rev* 94: 909-950, 2014.
48. Buchet K and Godinot C: Functional F1-ATPase essential in maintaining growth and membrane potential of human mitochondrial DNA-depleted rho degrees cells. *J Biol Chem* 273: 22983-22989, 1998.



This work is licensed under a Creative Commons Attribution-NonCommercial-NoDerivatives 4.0 International (CC BY-NC-ND 4.0) License.